**Earth Surface Processes and Landforms**
*Earth Surf. Process. Landforms* **33**, 123–141 (2008)
Published online 8 August 2007 in Wiley InterScience
(www.interscience.wiley.com) **DOI:** 10.1002/esp.1535

# Modeling the spatial distribution of landslide-prone colluvium and shallow groundwater on hillslopes of Seattle, WA†

William H. Schulz,* David J. Lidke and Jonathan W. Godt
*United States Geological Survey, Denver, CO, USA*

**Correspondence to: W. H. Schulz, Box 25046, MS-966, Denver, CO 80225, USA.*
*E-mail: wschulz@usgs.gov*


Received 24 March 2006;
Revised 4 April 2006;
Accepted 16 April 2006

## Abstract

**Landslides in partially saturated colluvium on Seattle, WA, hillslopes have resulted in property damage and human casualties. We developed statistical models of colluvium and shallow-groundwater distributions to aid landslide hazard assessments. The models were developed using a geographic information system, digital geologic maps, digital topography, subsurface exploration results, the groundwater flow modeling software VS2DI and regression analyses. Input to the colluvium model includes slope, distance to a hillslope–crest escarpment, and escarpment slope and height. We developed different statistical relations for thickness of colluvium on four landforms. Groundwater model input includes colluvium basal slope and distance from the Fraser aquifer. This distance was used to estimate hydraulic conductivity based on the assumption that addition of finer-grained material from downsection would result in lower conductivity. Colluvial groundwater is perched so we estimated its saturated thickness. We used VS2DI to establish relations between saturated thickness and the hydraulic conductivity and basal slope of the colluvium. We developed different statistical relations for three groundwater flow regimes. All model results were validated using observational data that were excluded from calibration. Eighty percent of colluvium thickness predictions were within 25% of observed values and 88% of saturated thickness predictions were within 20% of observed values. The models are based on conditions common to many areas, so our method can provide accurate results for similar regions; relations in our statistical models require calibration for new regions. Our results suggest that Seattle landslides occur in native deposits and colluvium, ultimately in response to surface-water erosion of hillslope toes. Regional groundwater conditions do not appear to strongly affect the general distribution of Seattle landslides; historical landslides were equally dispersed within and outside of the area potentially affected by regional groundwater conditions. Published in 2007 by John Wiley & Sons, Ltd.**

**Keywords: colluvium; landslide; coastal bluff; landscape development; groundwater**

## Introduction

Damaging and deadly landslides have been a recurring hazard in Seattle, WA, since at least the late 19th century (Laprade *et al.*, 2000; Coe *et al.*, 2004). Regional landslide hazard mitigation efforts may be guided by results of regional slope-stability assessments, some of which have been undertaken for Seattle (Montgomery *et al.*, 2001; Godt, 2004). Regional slope-stability assessments benefit from accurate representation of conditions responsible for landslide formation. Most Seattle landslides occur in partially saturated colluvium (see, e.g., Miller, 1973; Tubbs, 1974; Galster and Laprade, 1991; Miller, 1991; Baum *et al.*, 1998; Laprade *et al.*, 2000); therefore, accurate slope-stability assessments for Seattle require accurate models of the distributions of colluvium and shallow groundwater. However, only a basic knowledge of these distributions exists. Colluvium in Seattle generally occurs as discontinuous lenses less than a few meters thick along coastal bluffs and hillslopes along drainages (Galster and Laprade, 1991; Troost *et al.*, 2005). Colluvial groundwater in Seattle is generally perched (Galster and Laprade, 1991) and recharged by seepage

from a regional aquifer and by infiltration of winter precipitation. We developed statistical models of the distributions and depths of colluvium and shallow groundwater for parts of Seattle to assist regional slope-stability assessments.

Process-based models of colluvium distribution have been developed (see, e.g., Dietrich *et al.*, 1995; Heimsath *et al.*, 1999, 2001; Roering *et al.*, 1999, 2001). These models are most applicable to soil-mantled, unglaciated landscapes underlain by strong bedrock and account for processes including biogenic activity, tree throw, animal and insect burrowing, rainsplash and soil creep but do not account for colluvium production by landsliding and slope wash. Models of colluvium distribution have also been generated by interpolating empirical data. Zhou and others (2003) modeled the colluvium distribution for a region dominated by stream dissection. Their modeling was performed with the assumption that the base of the colluvium corresponded to streambed elevation; streambed elevations were defined in a geographic information system (GIS) and used to interpolate an estimated colluvium base using kriging. Craddock (1999) used water well data in a GIS to model the topography of bedrock buried beneath alluvium and colluvium. He used inverse distance weighting to interpolate the bedrock surface between data points and reported reasonable accuracy in model results.

Groundwater conditions of the Seattle area (Vaccaro *et al.*, 1998) and many other regions have been modeled, but these efforts generally addressed regional groundwater flow in aquifers of significant extent. Some regional slope-stability models include various approaches to model groundwater distributions in surficial soils (see, e.g., Montgomery and Dietrich, 1994; Dietrich *et al.*, 1995; Montgomery *et al.*, 1998; Baum *et al.*, 2002), but no studies were identified that included testing groundwater model results with observational data.

Although previous models for colluvium and shallow groundwater exist, they are not necessarily well suited for Seattle. The process-based models of colluvium formation are considered most applicable to slopes within drainage valley networks in unglaciated terrain where soil overlies strong rock (see, e.g., Dietrich *et al.*, 1995; Roering *et al.*, 1999) but Seattle is a geologically immature, recently glaciated area in which coastal erosion has been the dominant landscape-modifying force since retreat of glacial ice (Shipman, 2004). Colluvium in Seattle is produced by landsliding, slope wash and creep (see, e.g., Galster and Laprade, 1991) but the process-based models do not account for landsliding and slope wash. Groundwater-modeling approaches used previously appear inappropriate for modeling Seattle's colluvial groundwater because of the discontinuous nature and highly variable thickness of the colluvium deposits, as well as the high variability in recharge and discharge. The availability of new, detailed topographic data, geologic maps and subsurface exploration data (over 36 000 exploration points in Seattle, http://geomapnw.ess.washington.edu/index.php) provided us with the opportunity to develop accurate, empirically based models of colluvium and shallow groundwater distributions. Initially, we interpolated models (using kriging) for part of Seattle in which a high density of empirical data was available; however, model results did not adequately represent the complex geometry of Seattle's colluvium deposits. We then developed relations describing colluvium and groundwater depth using data for the Seattle southwest quadrangle and rule-based schemes, regression analysis and groundwater flow model simulations (VS2DI – Hsieh *et al.*, 2000). The relations were calibrated with empirical data from the Seattle southwest quadrangle and then applied over both the Seattle southwest and northwest quadrangles. The results were validated with empirical data from both quadrangles; Seattle southwest quadrangle data used for validation was not used during calibration. Validation indicated that the models accurately portray the distributions of colluvium and groundwater. Thus, our modeling approach should prove useful for regional slope-stability assessments in Seattle and in similar geologic regions. To permit application of the models to other regions, the relations we developed should be recalibrated using empirical data specific to those regions.

## Topography and geology of Seattle

Seattle occupies an isthmus between Puget Sound and Lake Washington (Figure 1). Landforms mainly result from Pleistocene glaciation, erosion by rivers and streams and erosion by wave action along the shorelines of lakes and the Puget Sound (Shipman, 2004). The area is characterized by rounded, elongate north–south trending hills and steep hillslopes above water bodies. Bluffs line most of the shoreline of Puget Sound and are the primary location of landslides in Seattle (Laprade *et al.*, 2000; Schulz, 2005, 2007). The bluffs rise 50–100 m above Puget Sound along most of the coastline and include vertical cliffs up to about 15 m high at hillslope crests. Bluff slopes are inclined about 30°, on average, though extensive areas more steeply inclined than 40° exist. The toe regions of most coastal bluffs in the study area are protected from wave action by manmade structures constructed during the early part of the 20th century. Some former coastal bluffs now appear as inland hills due to extensive grading operations (e.g. in the Interbay area, Figure 1). Steep, landslide-prone hillslopes with similar morphology to the coastal bluffs also occur along drainages and former glacial meltwater bodies (both streams and lakes). In our study area, for example, a steep hillslope is located along a former glacial lake shoreline about 500–640 m east of Point Williams (Figure 1).

Surficial geology of the Seattle area is primarily the result of Pleistocene glaciation and shoreline and fluvial processes that followed glacial retreat (see, e.g., Waldron *et al.*, 1962; Booth *et al.*, 2000; Troost *et al.*, 2005). The

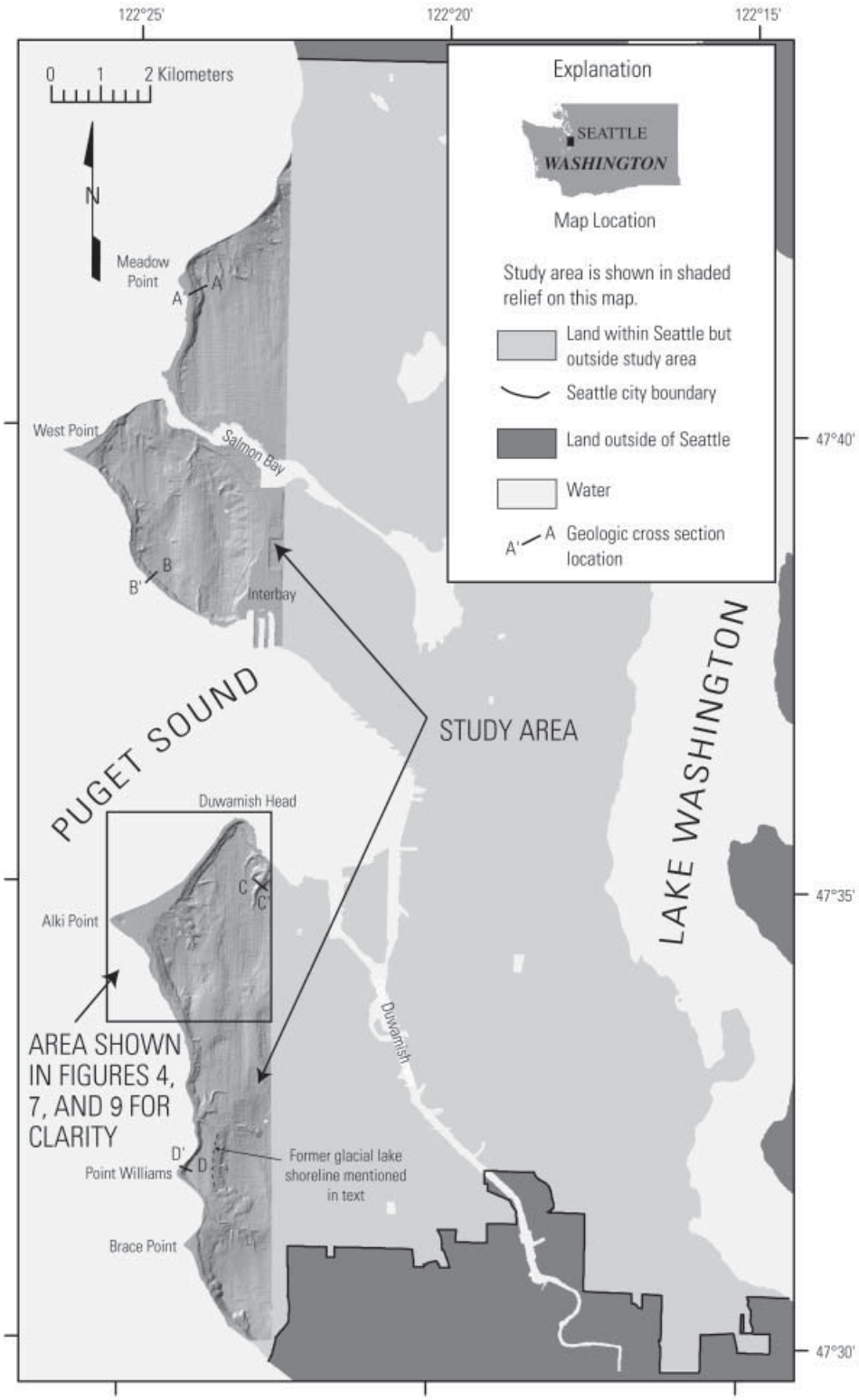


**Figure 1.** Map showing locations of study area (shaded relief), geologic cross-sections (Figure 10), and part of the study area shown for clarity in enlarged views (Figures 4, 7 and 9).

majority of exposed glacial and interglacial deposits result from the Vashon stade of the Fraser glaciation (16 400–17 400 yr B.P., Booth *et al.*, 2005). These deposits include, from oldest to youngest, Lawton Clay, advance outwash, till and recessional outwash. The older Olympia beds and pre-Olympia deposits underlie Lawton Clay and advance outwash, and are locally exposed in the lower parts of hillslopes. Lawton Clay consists of laminated to massive silt, clayey silt and silty clay deposited in lowland or proglacial lakes. Lawton Clay may be over 30 m thick and is generally exposed in the lower part of hillslopes. Advance outwash typically consists of fine sand deposited by proglacial meltwater streams, is locally as thick as about 60 m and generally forms the upper part of Seattle hillslopes. Vashon till is typically a very dense, poorly sorted, thin, discontinuous deposit containing variable amounts of clay, silt, sand, gravel and boulders. Recessional outwash generally occurs as discontinuous, thin deposits of sand and silt, but also includes laminated silt and clay deposits formed in glacial lake beds. Olympia beds and pre-Olympia deposits are very dense and hard, reach indeterminate thickness and may be exposed near the base of hillslopes.

### Hydrogeology of Seattle

Groundwater in the study area is generally perched on the Lawton Clay in the advance outwash (Newcomb, 1952; Vaccaro *et al.*, 1998). The Fraser aquifer, as defined by Vaccaro and others (1998), consists of the advance outwash and overlying till. A deeper aquifer also exists in parts of the pre-Olympia and Olympia beds (Vaccaro *et al.*, 1998), but generally has little effect on colluvial groundwater because it occurs at about sea level and below. Groundwater in the Fraser aquifer primarily flows laterally toward the coastal bluffs and hillslopes along drainages, although leakage occurs into the Lawton Clay, Olympia beds and pre-Olympia deposits (Newcomb, 1952; Vaccaro *et al.*, 1998). Where it encounters hillslopes, groundwater perched in the Fraser aquifer discharges either into overlying colluvial deposits or onto the ground surface in the form of broad seepage zones and concentrated springs. Woodward and others (1995) estimated groundwater discharge of 263 $m^3$ per day per km for coastal bluffs north of the study area. Groundwater that discharges into colluvial deposits remains perched on underlying strata with lower permeability (Galster and Laprade, 1991), or flows into underlying strata with similar or higher permeability.

The Lawton Clay and pre-Vashon deposits generally have the lowest hydraulic conductivity of geologic units in the study area. Savage and others (2000) provide a range of $1{\cdot}2 \times 10^{-10}$–$1{\cdot}2 \times 10^{-6}$ m/s for Lawton Clay and pre-Vashon deposits, and a range of $1{\cdot}2 \times 10^{-11}$–$1{\cdot}2 \times 10^{-4}$ m/s for till. Vaccaro and others (1998) provide hydraulic conductivity values of $1{\cdot}4 \times 10^{-4}$ m/s for advance outwash and $8{\cdot}5 \times 10^{-4}$ m/s for recessional outwash. No published hydraulic conductivity values were identified for the beach deposits in the area, but they likely are similar to those of the recessional outwash deposits because they are both generally unconsolidated coarse sand deposits. Simulated Seattle-area colluvium samples prepared and tested in a laboratory had hydraulic conductivity values that ranged from $1{\cdot}0 \times 10^{-5}$ to $1{\cdot}3 \times 10^{-3}$ m/s (Godt *et al.*, 2003). Several *in situ* hydraulic conductivity measurements were made in Seattle colluvium using a Guelph permeameter and obtained values of $3{\cdot}0$–$6{\cdot}0 \times 10^{-5}$ m/s (this study and Godt, 2004).

## Conceptual Model of the Spatial Distribution of Colluvium

Colluvium, as used herein, refers to loose, heterogeneous regolith deposits formed by biologic activity, pedogenic processes, slope wash, creep and landslides. Our observations suggest that colluvium on Seattle hillslopes primarily consists of landslide deposits. Galster and Laprade (1991) indicate that colluvium in Seattle is emplaced by landsliding, slope wash and soil creep.

Most colluvium-mantled hillslopes in Seattle are coastal bluffs. Coastal bluff formation in the area has been driven by sea-level rise (Downing, 1983; Booth, 1987; Terich, 1987; Shipman, 2004; Schulz, 2004, 2005, 2007). Sea level in the Seattle area rose rapidly following retreat of glacial ice; about 6–10 m of rise has occurred during the past 5000 years (Booth, 1987, Figure 7; Sherrod *et al.*, 2000). Although sea level rise continues, this rise no longer results in erosion of most Seattle bluff toes due to construction of shoreline protection, but the effects of bluff-toe erosion are still apparent in the distributions of colluvium and landslides, including very recent landslides (Schulz, 2005, 2007).

Formation of colluvium on eroding coastal bluffs is a cyclic process (see, e.g., Quigley *et al.*, 1977; Edil and Vallejo, 1980; Buckler and Winters, 1983; Vallejo and Degroot, 1988; Gerstel *et al.*, 1997; Hampton *et al.*, 2004; Schulz, 2005). Figure 2 provides a simplified depiction of this process on Seattle coastal bluffs. The sizes of the slope failures in the figure are exaggerated for clarity. Erosion of bluff toes by wave action causes oversteepening of the lower parts of bluffs, ultimately resulting in landslides. Landslides occur both in colluvium and underlying geologic units by fall, topple or sliding, and form colluvial deposits downslope and oversteepened areas upslope. Landslide locations progressively move upslope due to removal of downslope support by previous failures; eventually, the bluff crest fails. Contemporaneously, colluvium and underlying native deposits near the shoreline are eroded by wave

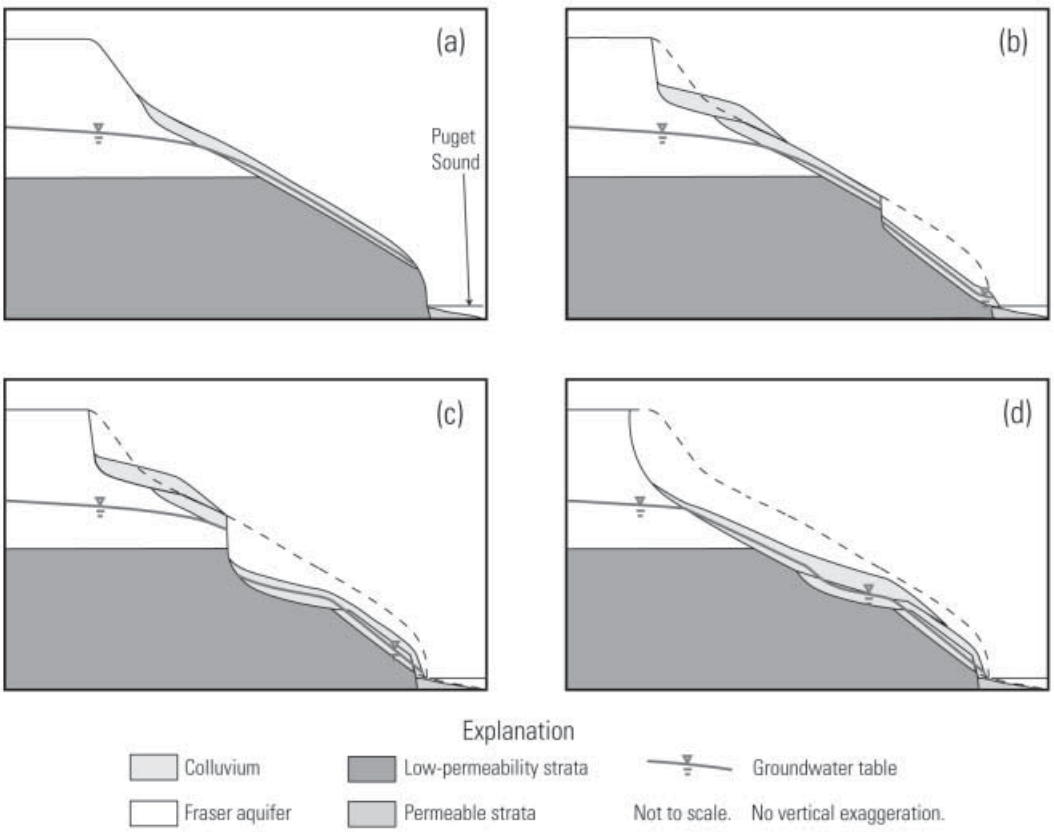


**Figure 2.** Conceptual model of colluvium development on Seattle coastal bluffs. (a) Wave action has eroded the lower part of the bluff and past landsliding has formed a relatively consistent colluvial mantle upslope. Both erosion and past landsliding have undermined upslope areas. Groundwater seepage from the Fraser aquifer charges the colluvium, as does precipitation (not shown). (b) Landslides occur at the bluff toe in response to erosion and at the hillslope crest in response to previous landsliding. The crest landslide involves only native deposits while the bluff toe landslide involves both colluvium and native deposits. New colluvium deposits are formed by both landslides. (c) Landsliding progresses in the upslope direction due to erosion by wave action and subsequent landsliding at the bluff toe. New landslide involves both native deposits and colluvium. (d) Landslide occurs at hillslope crest in native deposits and colluvium in response to undermining by landslides located downslope. New colluvium deposits are formed.

action, which undermines the hillslope anew. The relatively continuous cycle of landslides and formation of colluvium deposits results in retreating bluffs with a generally consistent cover of colluvium. It has been estimated that 150–900 m of bluff retreat has occurred along the Seattle Puget Sound coast during the last 5000 years (Galster and Laprade, 1991). Our observations and subsurface exploration reports indicate that as the relative rate of bluff retreat increases bluffs become steeper and have thinner colluvial cover. Areas with higher retreat rate also have higher, steeper escarpments at the slope crest.

Seattle hillslopes may be classified as either generally planar or benched, and characterized by four different landforms. We assumed a systematic variation of colluvium thickness based on these four landforms (Figure 3): (1) escarpment; (2) bench; (3) downslope of bench and (4) planar slope. Because escarpments are the upslope limit of colluvium production, we assumed that colluvium pinches out on escarpments in the upslope direction and that its thickness is proportional to position along the escarpment from top to bottom (as well as proportional to local slope). Downslope from the escarpment, colluvium thickness should increase with distance to some point, beyond which it would decrease. Thickening would be due to addition of colluvium from larger upslope areas as one progresses downslope, and thinning would be due to removal of colluvium near slope toes by erosion and landsliding. Based on our observations of relative apparent bluff retreat rate, escarpment characteristics and colluvium thickness, we assumed that colluvium is thinner downslope from higher, steeper escarpments and thicker downslope from shorter, flatter escarpments. Colluvium deposits downslope of benches were assumed to generally consist of wedges that thin

Published in 2007 by John Wiley & Sons, Ltd.

DOI: 10.1002/esp

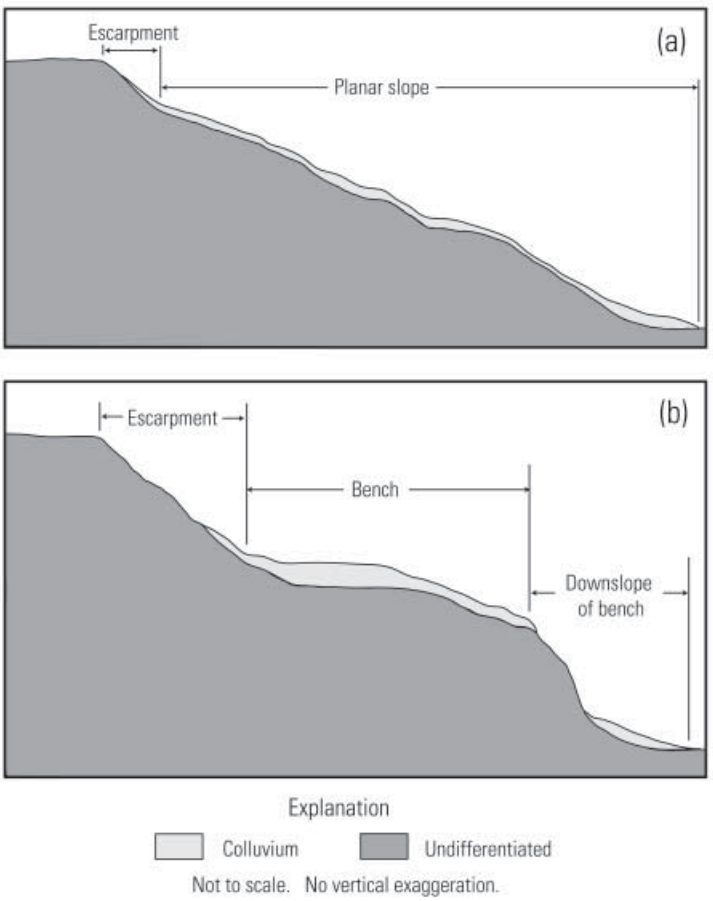


**Figure 3.** Cross-sections showing hillslope landforms common to Seattle and typical colluvium deposits on the landforms. Hillslopes have a crest escarpment that is steeper than areas located immediately downslope. (a) Planar slopes are generally consistently inclined downslope of the hillslope crest escarpments. (b) Benched slopes occur downslope of the hillslope crest escarpments and are subhorizontal to gently inclined. Hillslopes are steeper downslope of the benches than on the benches.

upslope. Since Seattle colluvium deposits form from gravity-driven processes, we assumed that colluvium deposits become thicker as slopes become flatter, regardless of landform. Finally, we assumed that colluvium extends no deeper than the local elevation of the bluff toe.

## Conceptual Model of the Spatial Distribution of Colluvial Groundwater

Colluvial groundwater in Seattle is generally perched and recharged by seepage from the Fraser aquifer and from precipitation. Therefore, colluvial groundwater depth should be proportional to position along the seepage face (from top to bottom) and should be least during the winter rainy season. On hillslopes absent Fraser aquifer seepage, recharge from precipitation was assumed to produce a colluvial water table subparallel to the base of the colluvium. Since colluvial groundwater is perched, its depth is dependent on colluvium thickness and saturated thickness of the colluvium. The colluvium basal slope is generally inclined at greater than 10° (assuming it is subparallel to the ground surface), so groundwater flow in colluvium is probably predominantly downhill and slope parallel, and the colluvium's saturated thickness is dependent on the basal slope of colluvium deposits and their hydraulic conductivity. Leakage to low-permeability strata underlying colluvium is probably insignificant. Groundwater discharges from colluvium at hillslope toes into underlying permeable strata or onto the ground surface if underlying strata are of low permeability. Groundwater also discharges on the ground surface where colluvium cannot transmit it at the rate supplied from upslope areas due to decreases in colluvium thickness, hydraulic conductivity or basal slope.

Published in 2007 by John Wiley & Sons, Ltd.

DOI: 10.1002/esp

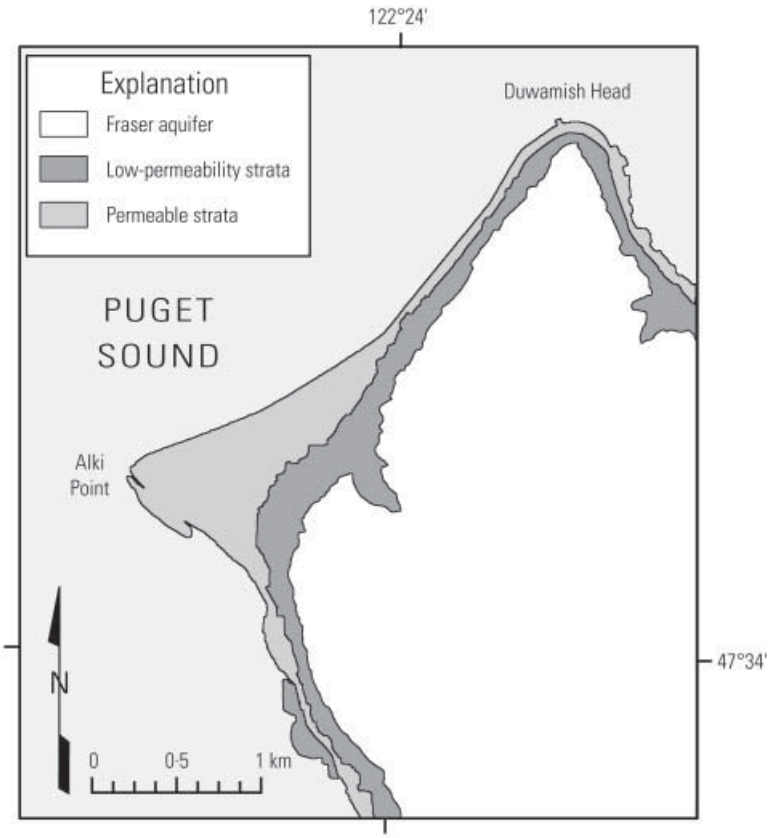


**Figure 4.** Hydrogeologic map generalized from Troost *et al.* (2005).

Colluvium is produced from each of the hydrogeologic units that comprise hillslopes. The uppermost unit in most of the study area is the advance outwash, which has greater hydraulic conductivity and generally coarser grain-size distribution than underlying units. Therefore, it is likely that colluvium hydraulic conductivity decreases downslope of the base of the advance outwash as finer-grained sediment is incorporated, as observed by Godt (2004, Figure 3).

Based on recent geologic mapping (Troost *et al.*, 2005), we identified three generalized hydrogeologic units that could affect colluvial groundwater. Figure 4 shows our generalized hydrogeologic map for part of our study area (only part is shown for clarity). This part includes the greatest spatial density of reported historical landslides in Seattle (Coe *et al.*, 2004). The generalized hydrogeologic units are (1) the Fraser aquifer (modified from Vaccaro *et al.*, 1998, by excluding Vashon till), (2) low-permeability strata (relative to adjacent strata) that underlie the Fraser aquifer and overlie it in thin, discontinuous deposits and (3) permeable strata that generally overlie both the Fraser aquifer and low-permeability strata. The Fraser aquifer consists of advance outwash; low-permeability strata include till, Lawton Clay, Olympia beds and pre-Olympia deposits. Permeable strata include beach deposits, alluvium and glacial recessional outwash. Related to our hydrogeologic map, we assumed a systematic variation of saturated thickness between three groundwater-flow regimes to account for our assumptions regarding colluvial groundwater recharge and discharge (Figure 5): (1) seepage regime, colluvium overlying the Fraser aquifer seepage face; (2) downslope-of-seepage regime, colluvium contiguous with colluvium located upslope in the seepage regime; (3) seepage-lacking regime, colluvium on hillslopes that lack Fraser aquifer seepage. The seepage-lacking regime includes those areas that are not contiguous with saturated colluvium located upslope.

## Data and Methods

We used a high-resolution (3 m) digital elevation model (DEM) generated from light detection and ranging (LIDAR) data and 1:12 000-scale geologic maps of the Seattle southwest and northwest quadrangles (Troost *et al.*, 2005). We obtained logs for 617 subsurface explorations that date to the mid-1900s (Kathy G. Troost, written communication,

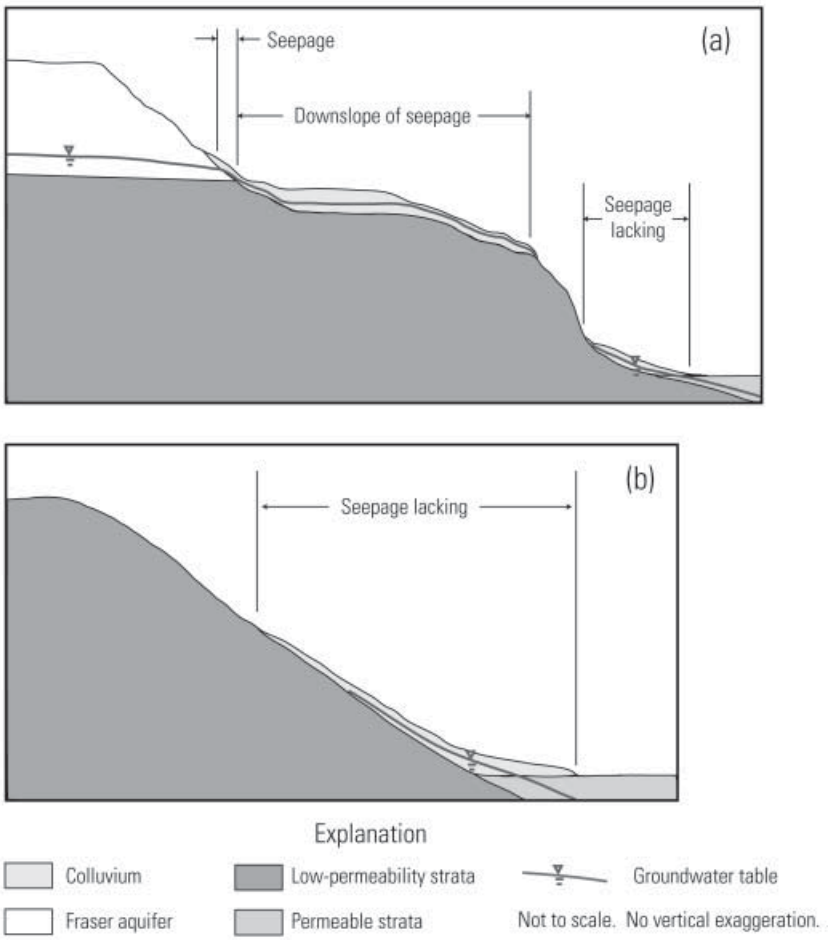


**Figure 5.** Cross-sections showing colluvial groundwater flow regimes common to Seattle. (a) The seepage regime occurs where colluvium overlies the Fraser aquifer seepage face, while the downslope-of-seepage regime occurs in colluvium deposits downslope of and contiguous with colluvium in the seepage regime. The seepage-lacking regime occurs in colluvium deposits that are not contiguous with colluvium in the seepage or downslope-of-seepage regimes. (b) The seepage-lacking regime also occurs on hillslopes absent the Fraser aquifer.

2003) and reviewed 184 exploration reports on file with the Washington Department of Ecology. Many of the reports we reviewed were for explorations performed where colluvium was absent so these were used to help delineate the overall distribution of colluvium. We created GIS databases of exploration results, including those that helped define the saturated thickness of the Fraser aquifer. We estimated colluvium and groundwater depths at each exploration site by constructing geologic cross-sections, thus also utilizing the findings at nearby explorations and ensuring consideration of local topographic and geologic conditions.

## The colluvium model

To develop the colluvium model, we generated relations individually between each independent variable (described below) and colluvium thickness observed at the subsurface exploration points used for calibration (40 points). Each of the individual relations was normalized by the maximum colluvium thickness value that resulted from the relation. The normalized relations were then combined to formulate the complete colluvium thickness relation, and weighting factors for each of the normalized relations were determined by systematic trial and error aided by regression analyses. Combination of the individual relations was guided by our conceptual model; functions of escarpment slope and height and of distance downslope from the escarpment are summed to provide the main input to the complete relation because they were thought to approximate the availability of colluvium related to the local, relative rates of slope

retreat and toe erosion. A function of slope modifies the escarpment- and distance-function sum because thicker colluvium occurs on lower slopes and thinner colluvium occurs on steeper slopes. We created functions independent of empirical data to account for our assumptions regarding colluvium depth at hillslope toes and within the escarpment area. Colluvium at hillslope toes does not extend to greater depth than the local elevation of the toe and on escarpments pinches out upslope at a location related to the overall escarpment slope.

To obtain values of independent variables used in calibrating the relations and producing the final model, we first delineated the four landforms in a GIS using cross-sections, slope and curvature gridded data sets (grids) calculated from the 3 m LIDAR DEM, the hydrogeologic map and the exploration point database as guides. We then constructed grids of the independent variables escarpment height and slope, distance from the escarpment base and top, topographic slope and elevation of the base of colluvium in the hillslope toe area. We compiled, in a spreadsheet, values for the independent variables at locations of calibration observations. Relations were then developed to predict colluvium thickness using these data, as described above. The relations were applied in the GIS to construct the model of colluvium distribution. The general form of the colluvium thickness expression for escarpment, bench and planar-slope landforms is

$$T_C = 21f(S)[1{\cdot}1f(S_E H_E) + 0{\cdot}1f(D_E)]A_E - T_D \quad (1)$$

where $T_C$ is the thickness of colluvium in meters, $f(S)$ is a function of topographic slope, $S$, $f(S_E H_E)$ is a function of the escarpment slope, $S_E$, and height, $H_E$, $f(D_E)$ is a function of distance downslope from the escarpment, $D_E$, $A_E$ is an adjustment for the escarpment landform and $T_D$ is the maximum depth of colluvium in hillslope toe areas. Figure 6 shows these parameters graphically with the exception of $A_E$; $A_E$ is dependent on $W_E$, $S_E$ and $H_E$ as described below.

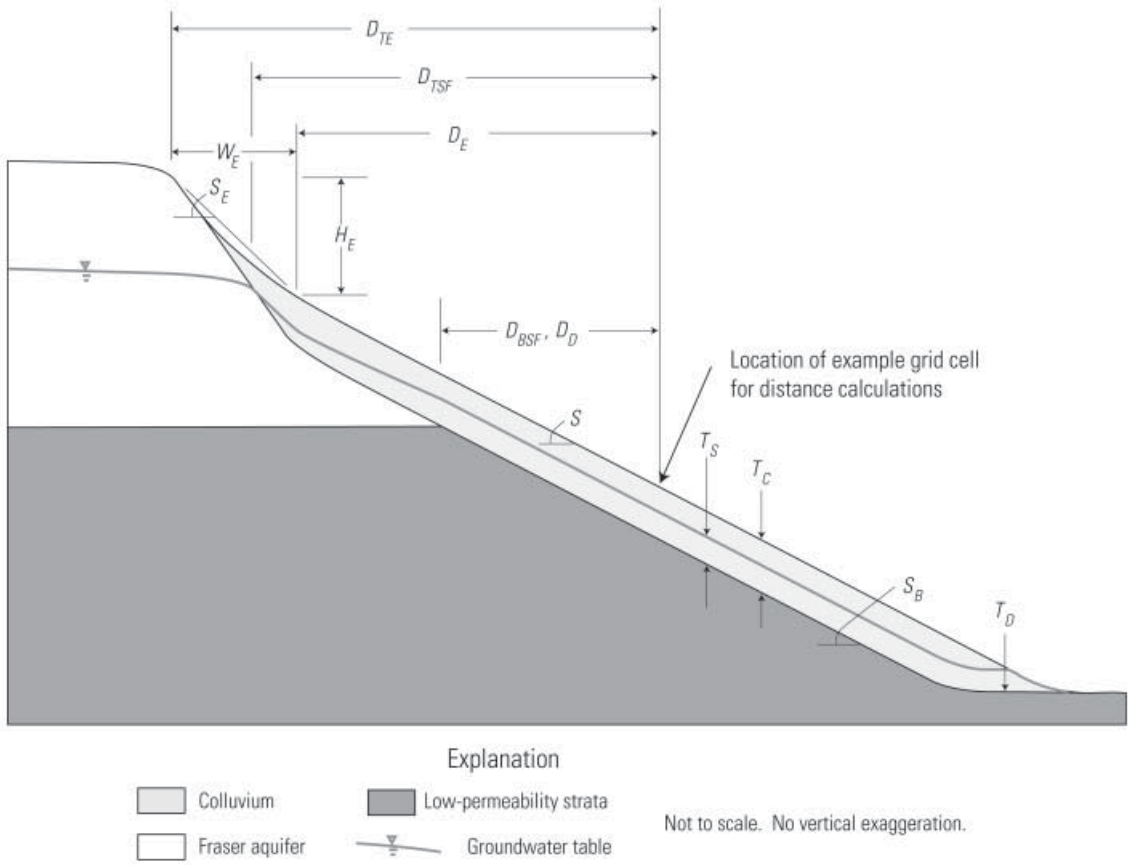


**Figure 6.** Cross-section showing parameters used in the colluvium and groundwater models. The cross-section is aligned along the average slope for the example hillside. Distance parameters $D_{TE}$, $D_{TSF}$, $D_E$, $D_{BSF}$ and $D_D$ are shown for an example grid cell and will have unique values for each grid cell located along the cross-section line. Values of $S$ and $S_B$ may also be unique for each grid cell located along the cross-section line, while values of $S_E$, $H_E$, $W_E$ and $T_D$ will be approximately the same for all grid cells along the cross-section line.

Published in 2007 by John Wiley & Sons, Ltd.


DOI: 10.1002/esp

The escarpment slope-height function has an order of magnitude greater importance than the escarpment distance function for estimating colluvium thickness, as indicated by the weighting factors applied to these functions (1·1 and 0·1, respectively).

Colluvium in downslope-of-bench landform areas was modeled as a wedge, which was represented by an expression of the form

$$T_C = f(S)f(E) - T_D \tag{2}$$

where $f(E)$ is a function of elevation, $E$, in meters. This expression was constructed so that elevation controlled the wedge geometry, in general, which was modified by the slope function. No subsurface observational data were available for this landform; our colluvium thickness expression was constructed to approximate conditions we observed on the ground surface.

*Topographic slope function.* Our observations and slope-stability modeling suggest that colluvium rarely occurs on slopes more steeply inclined than about 45°. A function of slope was developed that fit the observational data well and did not predict colluvium on slopes more steeply inclined than 46·5°:

$$f(S) = 0{\cdot}305 - 6{\cdot}55 \times 10^{-3} S \qquad \text{for } S \le 46{\cdot}5° \text{ and} \tag{3}$$

$$f(S) = 0 \qquad \text{for } S > 46{\cdot}5°.$$

This equation predicts thinner colluvium on steeper slopes and thicker colluvium on flatter slopes.

*Escarpment slope-height function.* Escarpment height was determined by comparing elevations of the escarpment top and bottom located nearest each grid cell. Escarpment slope was calculated from height and width, which was determined by comparing horizontal distances to the escarpment top and bottom located nearest each grid cell. Relations between colluvium thickness and escarpment height and slope were developed considering the bench landform independent of the escarpment and planar-slope landforms.

Bench landform:

$$f(S_E H_E) = -6{\cdot}36 \times 10^{-5} S_E H_E + 0{\cdot}875 \qquad \text{for } S_E H_E \le 13\,762{\cdot}6 \text{ and} \tag{4}$$

$$f(S_E H_E) = 0 \qquad \text{for } S_E H_E \ge 13\,762{\cdot}6.$$

Escarpment and planar-slope landforms:

$$f(S_E H_E) = -1{\cdot}09 \times 10^{-4} S_E H_E + 0{\cdot}986 \qquad \text{for } S_E H_E \le 9045{\cdot}9 \text{ and} \tag{5}$$

$$f(S_E H_E) = 0 \qquad \text{for } S_E H_E \ge 9045{\cdot}9.$$

Both equations predict thicker colluvium downslope from shorter, flatter escarpments and thinner colluvium downslope from higher, steeper escarpments.

*Distance-from-escarpment function.* Relations between distance from the escarpment and colluvium thickness were developed considering the bench landform independent of the escarpment and planar-slope landforms.

Bench landform:

$$f(D_E) = 6{\cdot}7 \times 10^{-4} D_E + 0{\cdot}675 \tag{6}$$

Escarpment and planar-slope landforms:

$$f(D_E) = -3{\cdot}75 \times 10^{-4} D_E + 0{\cdot}862 \tag{7}$$

Equation (6) predicts thicker colluvium with increasing distance from the escarpment, while Equation (7) predicts thinner colluvium with increasing distance from the escarpment.

*Elevation function.* The relation between elevation (meters) and colluvium thickness for the downslope-of-bench landform that produced acceptable deposit geometry was

$$f(E) = -0{\cdot}105E + 5{\cdot}649 \qquad \text{for } E \le 53{\cdot}8 \text{ and} \tag{8}$$

$$f(E) = 0 \qquad \text{for } E > 53{\cdot}8.$$

This equation predicts colluvium to thin and pinch out in an upslope direction.

*Escarpment landform adjustment.* The upslope limit of colluvium within the escarpment landform was estimated by assuming that precipitous escarpments (overall inclination steeper than 70°) entirely lack colluvium and gently sloping escarpments (overall inclination flatter than 25°) have colluvial deposits that extend to the escarpment top. For escarpments with overall inclination between 25 and 70°, we assumed a linear variation in the location of the upslope deposit terminus:

$$\begin{gathered}\text{for } S_E > 70^\circ \\ A_E = 0 \\ \text{for } S_E < 25^\circ \\ A_E = D_{TE}/W_E \\ \text{for } 25^\circ \le S_E \le 70^\circ \\ A_E = (D_{TE} - W_E + (-W_E S_E/45 + 1{\cdot}56W_E))/(-W_E S_E/45 + 1{\cdot}56W_E)\end{gathered} \tag{9}$$

where $D_{TE}$ is distance to the escarpment top and $W_E$ is escarpment width. Equation (3) accounts for local slope variation and results in a predicted absence of colluvium anywhere that slope exceeds 46·5°; escarpments with overall inclination less than 70° will have predicted colluvium deposits where local slope does not exceed 46·5°.

*Toe depth adjustment.* The location of the toe of colluvium deposits was delineated manually in the GIS based on slope and geology. This location was then converted to a grid with values of ground surface elevation, and these elevations were projected in the upslope direction beneath predicted colluvium deposits. We adjusted calculated colluvium thicknesses for grid cells near the deposit toe by limiting the maximum colluvium depth to the elevations in the grid.

## The groundwater model

We developed relations to estimate saturated thickness using methods similar to those used to estimate colluvium thickness. The variably saturated groundwater flow model VS2DI (Hseih *et al.*, 2000) was used to analyze the variations of saturated thickness with hydraulic conductivity and basal slope of colluvium, as described below. These relations were normalized and combined in the colluvial groundwater expression with relations that account for the conditions in our conceptual model, including a best-fit relation between distance downslope from the advance outwash and hydraulic conductivity and geometric relations we developed independent of empirical data. The geometric relations force groundwater depth in colluvium overlying the seepage face to scale linearly with distance downslope from the top of the seepage face, colluvium on hillslopes absent Fraser aquifer seepage to retain groundwater with a depth that scales linearly with distance downslope from the top of the colluvium deposit and groundwater to drain to permeable strata if these strata underlie the colluvium deposit toe or groundwater to remain perched if low-permeability strata underlie the toe. The final saturated thickness relation was developed by combining the individual relations and iteratively solving for two constants summed to represent recharge; one constant represents recharge present year round and the second represents additional recharge present during the winter. The final recharge constants produced best fits between observed (39 observations) and predicted saturated thickness values.

To develop the colluvial groundwater model, the seepage face on the Fraser aquifer was approximated in the GIS using water levels observed in the Fraser aquifer (42 observations). Next, the three groundwater flow regimes were delineated using slope and curvature grids and the colluvium model results. We then developed relations between observed values of saturated colluvium thickness and the independent variables, assisted by regression analysis. The final saturated thickness results were subtracted from the colluvium thickness results to derive the groundwater depth model. Only a model of wet season conditions is presented here; however, dry season conditions can be estimated by omitting a wet-season recharge factor. The general form of the equation used to model groundwater in colluvium was

$$T_S = f(S_B) f(K)(r + w_r) A_{SF} A_{AS} - A_T \tag{10}$$

where $T_S$ is the saturated thickness of colluvium in meters, $f(S_B)$ is a function of colluvium basal slope, $S_B$ (Figure 6), $f(K)$ is a function of saturated hydraulic conductivity, $K$, $r$ is a regime-variable constant representing groundwater recharge from the Fraser aquifer and remnant groundwater from previous wet seasons, $w_r$ is a constant representing groundwater recharge from precipitation and increased recharge from the Fraser aquifer during the winter rainy season, $A_{SF}$ adjusts the amount of recharge to colluvium that overlies the Fraser aquifer seepage face, $A_{AS}$ is an adjustment made for hillslopes absent recharge from Fraser aquifer seepage and is equivalent to $A_E$ (Equation (9)) and $A_T$ is an adjustment made in colluvium toe areas.

*Slope of colluvium base and hydraulic conductivity of colluvium functions.* We used VS2DI (Hsieh *et al.*, 2000) to develop simplified relations between saturated thickness and the basal slope and hydraulic conductivity of colluvium. Vertical cross-sections were created in VS2DI to simulate colluvium as an aquifer overlying an inclined impermeable boundary. Free seepage boundaries were assigned to the upper surface and downslope aquifer terminus, which represent the top of colluvium and the colluvium toe overlying a similarly permeable material, respectively. A vertical flux boundary was established along the upslope terminus of the colluvial aquifer to simulate recharge from the Fraser aquifer. Various simulations were run through sufficient time steps to reach equilibrium conditions. These simulations included constant hydraulic conductivity of $1.4 \times 10^{-4}$ m/s with basal slopes of 4, 10, 20, 30, 40 and 50°, and constant basal slope of 30° and hydraulic conductivity that varied from $1 \times 10^{-5}$ to $1 \times 10^{-2}$ m/s in $10^1$ increments. Saturated thicknesses were determined from model output. Hydraulic conductivity, $K$, and resulting saturated thickness values were best fit by the relation (normalized by maximum value)

$$f(K) = 2{\cdot}974 \times 10^{-3} K^{-0{\cdot}5745} \tag{11}$$

where $f(K)$ is saturated thickness (m) relative to $K$.

Basal slope, $S_B$, and calculated saturated thickness values obtained using VS2DI were best fit by the normalized relation

$$f(S_B) = 1 - 0{\cdot}0153 S_B \tag{12}$$

where $f(S_B)$ is saturated zone thickness (m) relative to $S_B$. During modeling, $S_B$ values were obtained by calculating a slope grid from a colluvium base DEM.

*Hydraulic conductivity function of distance.* The following relations were developed to predict colluvium hydraulic conductivity by iteratively solving the saturated thickness relations while systematically varying minimum and maximum $K$, the distance beyond which $K$ decreases and the distance beyond which $K$ is minimum until best fits were obtained between observed and calculated saturated thicknesses.

Seepage-lacking regime:

$$K = 4 \times 10^{-5} \text{ m/s} \tag{13}$$

Seepage and downslope-of-seepage regimes:

$$\begin{aligned} K &= 4 \times 10^{-5} \text{ m/s} && \text{for } D_D \geq 122 \text{ m}, \\ K &= 1 \times 10^{-4} \text{ m/s} && \text{for } D_D \leq 23 \text{ m, and} \\ K &= 1{\cdot}23 \times 10^{-4} - 3{\cdot}08 \times 10^{-7} D_D && \text{for } 23 \text{ m} < D_D < 122 \text{ m} \end{aligned} \tag{14}$$

where $D_D$ is distance downslope of the Fraser aquifer (Figure 6). The $K$ values used in the model generally agree with those we measured *in situ* ($3-6 \times 10^{-5}$ m/s).

*Groundwater recharge factors.* The groundwater recharge factors $r$ and $w_r$ were determined by iteratively solving the saturated thickness relations (10) through (14) while systematically varying these factors and performing regression analysis to determine the best correlation between calculated and observed saturated thickness values. The factor $w_r$ was used to adjust dry season water level observations by comparing adjusted values to solutions for wet season observations; thus it approximates an average saturated thickness variation from dry to wet season (observations were made over 54 years). The value of $w_r$ that provided best fits between observed and estimated saturated thicknesses was 1·52. The factor $r$ was permitted to vary between groundwater flow regimes. The best-fit value of $r$ was 3·78 for the downslope-of-seepage and seepage regimes, and 1·77 for the seepage-lacking regime.

*Seepage face adjustment.* We assumed that the amount of groundwater recharge to colluvium that overlies the Fraser aquifer seepage face (seepage regime) was directly proportional to position relative to the top and bottom of the seepage face. Based on this assumption, the calculated saturated thickness at each grid cell located within the seepage face area was adjusted by the equation

$$A_{SF} = D_{TSF}/(D_{TSF} + D_{BSF}) \tag{15}$$

where $D_{TSF}$ and $D_{BSF}$ are distances to the top and bottom of the seepage face, respectively (Figure 6).

To provide the parameters necessary to calculate the seepage face adjustment, the seepage face was modeled using saturated thicknesses observed within the Fraser aquifer. To do so, we first calculated an elevation grid of the contact

between the Fraser aquifer and underlying low-permeability strata beneath the modeled colluvium. We then interpolated the observed saturated thickness point values to a continuous grid with the same geometry as the Fraser aquifer/low-permeability strata contact elevation grid. We summed these two grids to calculate a top elevation of the seepage face grid. We then projected the top elevations of the seepage face to the hillsides. Finally, these top elevations were compared with the elevations of the colluvium base to establish the location of the seepage face top. The parameter $D_{BSF}$ was calculated during the process. $D_{TSF}$ was calculated using the domain defined by the Fraser aquifer/low-permeability strata contact elevation grid and the seepage face top location.

We evaluated whether the Fraser aquifer saturated thickness model correlated with observed colluvium saturated thicknesses downslope of the seepage face. No correlation was observed, so we only included a seepage face adjustment for the seepage regime.

*Toe discharge adjustment and depth to groundwater.* To represent our assumed discharge conditions at hillslope toes, we developed a modified colluvium thickness grid that includes initially calculated colluvium thicknesses (pre-toe adjustment) for areas where colluvium overlies permeable strata and final calculated colluvium thicknesses (toe adjusted) where colluvium overlies low-permeability strata. The groundwater-depth model was generated by subtracting the saturated thicknesses from this modified colluvium thickness grid.

## Results

### The colluvium model

Some of the colluvium thickness model results are shown in Figure 7. Deposits reach a maximum thickness of 7·4 m and have an average thickness of 2·7 m. Thick deposits are most extensive on the gentle hillslopes east of Alki Point and in the axes of drainages.

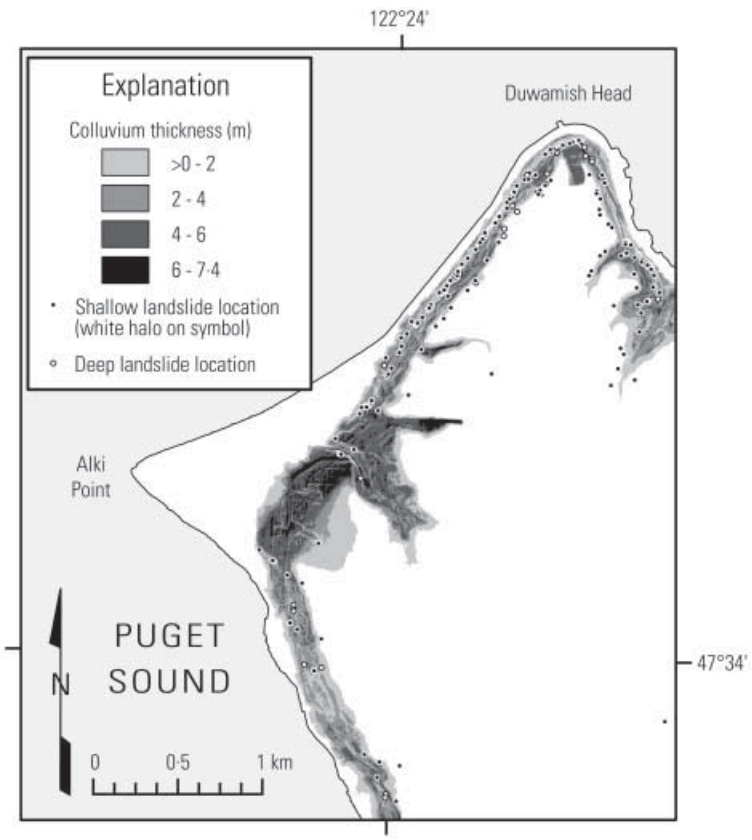


**Figure 7.** Map showing some of the colluvium model results for Seattle. Locations of historical deep and shallow landslides (modified from Laprade *et al.*, 2000) are also shown.

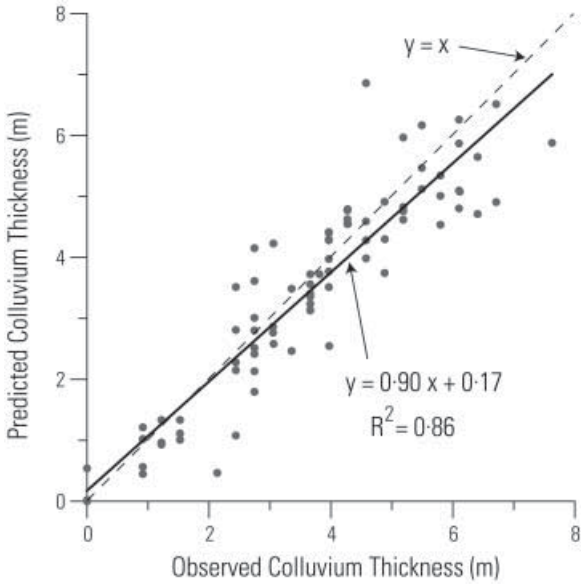


**Figure 8.** Plot showing observed colluvium thickness versus model results.

Eighty-five colluvium thickness observations (37 and 48 from the southwest and northwest quadrangles, respectively) were used to validate the model. None of these values were used during calibration; calibration only used values from the southwest quandrangle so the northwest quadrangle values provide model verification for a second, similar region. Figure 8 is a plot of observed colluvium thickness values versus model-predicted values. The values are best fit by a linear relation with a slope of 0·90, *y*-intercept of 0·17 and root-mean-square value of 0·86. This best-fit relation indicates that, in general, the model slightly over-predicts colluvium thickness for areas where actual colluvium thickness is less than 1·7 m and under-predicts colluvium thickness for areas where actual colluvium thickness is greater than 1·7 m.

## The groundwater model

Part of the wet-season groundwater depth model is shown in Figure 9. Groundwater depth averages 1·2 m and has a maximum of 7·0 m. Several geologic cross-sections (locations shown in Figure 1) were generated directly from the colluvium and groundwater model results. Cross-sections A–A′, B–B′ and D–D′ (Figure 10) are normal to coastal bluffs. Cross-section C–C′ (Figure 10) is normal to the axis of a drainage, indicating the utility of the models on hillslopes other than coastal bluffs.

Seventeen saturated thickness observations made during the wet season were used to validate our wet-season groundwater model. These observations were not used during calibration and include values from the northwest quadrangle, for which no calibration was performed. Figure 11 shows a plot of these observed values versus predicted values, which are best fit by a linear relation with a slope of 0·90, *y*-intercept of 0·21 and root-mean-square value of 0·97. The best-fit relation indicates that, in general, the model slightly over-predicts saturated thickness for areas where actual saturated thickness is less than 2·1 m and under-predicts saturated thickness for areas where actual saturated thickness is greater than 2·1 m. We also validated the groundwater model using water levels observed outside of the winter wet season for which our model was created. The non-wet- (dry-) season water level observations were adjusted by our wet-season recharge factor, $w_r$, which introduces error in our validation results. Figure 11 shows the adjusted observed dry-season values versus predicted wet-season values. As expected, inclusion of adjusted observed dry-season values reduces the level of correlation between predicted and observed values; all data (wet season plus adjusted dry season) are best fit by a linear relation with a root-mean-square value of 0·89.

## Historical landslide locations and the colluvium and groundwater models

Laprade and others (2000) compiled a database of 1326 historical landslides that have been reported in Seattle since the 1890s. Of these landslides, 596 were reported within our study area, and 77% of these were located within our

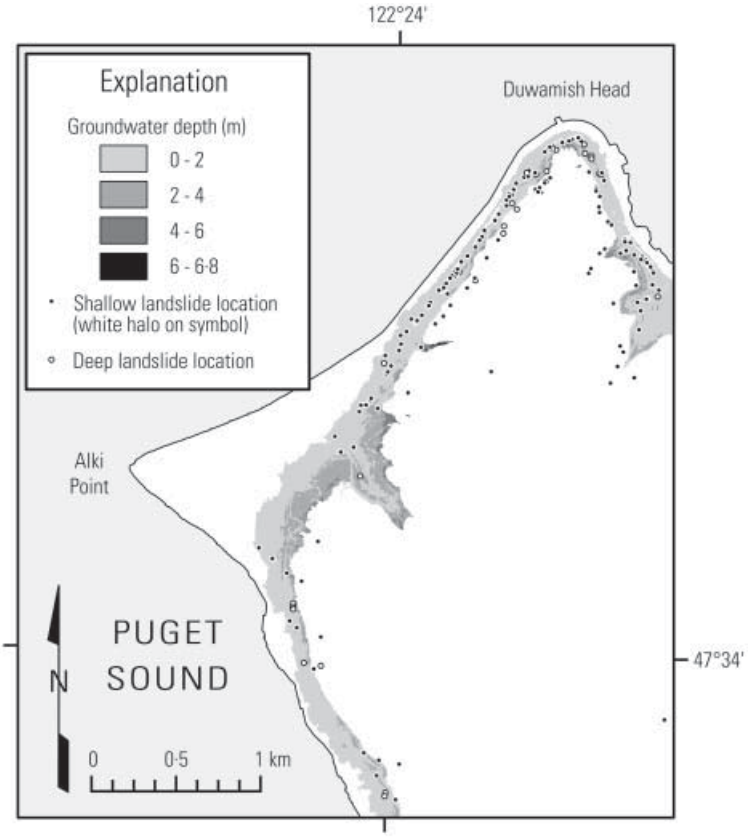


**Figure 9.** Map showing colluvial groundwater model results and locations of historical deep and shallow landslides (modified from Laprade *et al.*, 2000) for part of Seattle.

modeled colluvium deposits. Five hundred and fifty-one landslides were of known depth; 80% were shallow (less than about 2 m deep, Laprade *et al.*, 2000), while 20% were deep (greater than about 2 m deep, Laprade *et al.*, 2000). Shallow landslides include those referred to in the historical landslide database as 'high bluff peeloffs' (Laprade *et al.*, 2000), which may be categorized more generally as falls and topples (Cruden and Varnes, 1996). Seventy-five percent of shallow landslides and 81% of deep landslides were located within the modeled colluvium deposits. Forty-eight percent of shallow landslides and 65% of deep landslides (51% in sum) were located within the predicted distribution of colluvial groundwater.

## Discussion

The models described herein provide reasonably accurate predictions of colluvium and groundwater depth, as indicated by Figures 8 and 11. Hence, our conceptual models of colluvium development and groundwater occurrence generally seem appropriate, as do our approaches to estimate the distributions of colluvium and groundwater. However, our assumptions regarding colluvium thickness related to distance downslope from the escarpment were incorrect, at least in part. Calibration showed that colluvium thickness continually increases on the bench landform and continually decreases on the planar slope landform, rather than increasing to some point and then decreasing, as we assumed would happen. No subsurface exploration data existed for the escarpment landform so we do not include it in this discussion. The constant increase on the bench landform suggests that colluvium deposits thereon are not subjected to progressive loss of colluvium that would be expected to result from toe erosion and multiple landslide events with different geometries and locations. These deposits are subjected to sudden, abrupt failure at their downslope ends due to landslide occurring primarily on the much steeper hillside located just downslope. We can not explain the constant decrease of colluvium thickness on the planar slope landform with distance from the escarpment. However, the weighting factor for the distance from the escarpment function indicates that it has little effect on colluvium

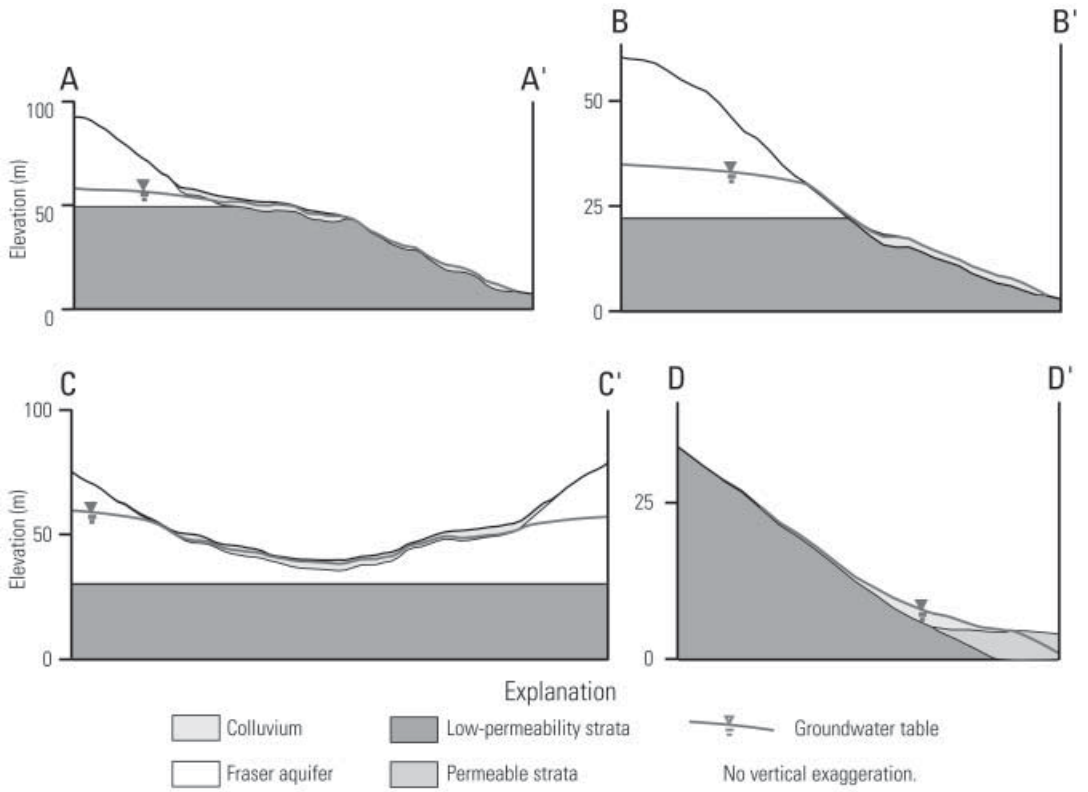


**Figure 10.** Geologic cross-sections drawn using a GIS showing colluvium, Fraser aquifer seepage face and colluvial groundwater model results. Cross-section locations are shown in Figure 1. The groundwater table shown within the Fraser aquifer and the base of this aquifer were added for illustration purposes. However, elevations of the intersections of the groundwater table and base of the Fraser aquifer with the base of colluvium were obtained directly from the Fraser aquifer seepage face model.

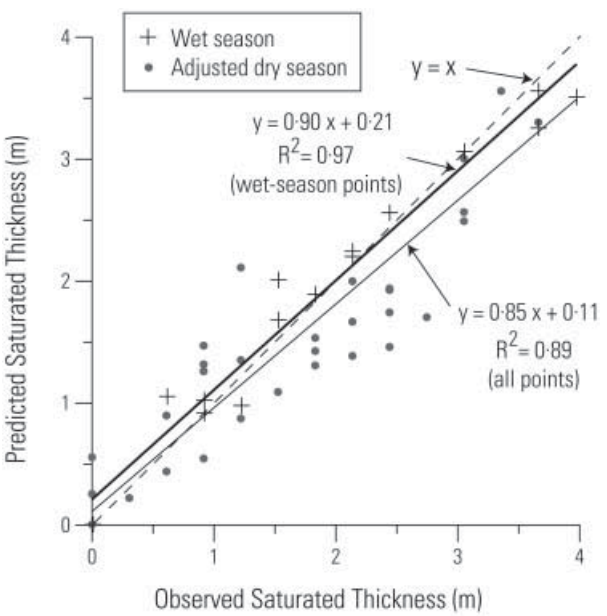


**Figure 11.** Plot showing observed colluvium saturated thickness versus model results. The model estimates winter wet-season water levels. Therefore, for use in this figure, dry-season observations were adjusted to approximate winter wet-season levels by adding the wet-season groundwater recharge constant $w_r$.

thickness. For example, Equation (7) results in a 3·9 cm reduction in predicted colluvium thickness for every 50 m downslope from the escarpment on a planar slope.

Roads and other areas of extensive grading are apparent in the models (Figures 7 and 9) because of their spatially consistent slope aspect and inclination. We attempted to develop automated methods to identify graded areas based on slope, aspect and curvature distributions and account for these areas in colluvium and groundwater-depth calculations but did not produce consistently favorable results. Similarly, our groundwater model does not directly account for human modifications to natural surface water and groundwater flow systems. However, the model does indirectly account for such modifications since it is primarily based on empirical data obtained after most modifications had been constructed. Results for both models correlate well with observed values (most of which were obtained in developed areas), suggesting that our models represent conditions adequately for regional slope-stability assessments.

### Colluvium and landslides

Our conceptual model of colluvium development requires that landslides occur in native deposits at hillslope crests free of colluvium, and in both colluvium and native deposits in downslope areas. Model results suggest that these conditions are present. Our analysis indicates that 25% of shallow and 19% of deep historical landslides occurred where colluvium is absent (see, e.g., Figure 7). Deep landslides are relatively more common than shallow landslides within colluvium deposits, as would be expected, and can more readily extend into underlying native deposits.

### Colluvial groundwater and landslides

As expected, deep landslides appear to have been more directly affected by regional groundwater conditions than shallow landslides, as suggested by the greater relative abundance of deep landslides (65%) than shallow landslides (48%) within the distribution of colluvial groundwater. The modeled colluvial groundwater distribution is dependent on the distribution of the Fraser aquifer seepage zone. Therefore, since about half the historical landslides occurred within the distribution of colluvial groundwater, landslides have been about equally as likely to occur with possible influence of groundwater from the Fraser aquifer as without. This finding contradicts the conclusion first made by Tubbs (1974, 1975) that the basal contact of the Fraser aquifer defines the location where Seattle landslides typically occur. Tubbs' conclusion has no direct role in our conceptual model of colluvium formation. The model assumes that colluvium forms largely from landslides and these occur in response to over-steepening of hillslope areas by fluvial and coastal erosion and landsliding located downslope. Our statistical model reflects these assumptions with the thickness of gravitationally transported colluvium dependent on slope and the prediction of thinner colluvium deposits and higher, steeper escarpments along more actively failing hillslopes. Our conceptual model agrees with recent findings that both prehistoric and historical landslides have only naturally occurred on Seattle hillslopes whose toes have been eroded, that only 29% of historical landslides occurred along the base of the Fraser aquifer as defined by Tubbs (1974, 1975) and that 64% of historical landslides occurred outside of areas possibly affected by Fraser aquifer seepage (Schulz, 2007). Seepage from the Fraser aquifer is only indirectly involved in our conceptual model of colluvium and colluvial groundwater in that it may affect landslide characteristics and frequency (and, hence, colluvium depth), but the seepage is not necessary for landslides to occur.

## Conclusions

We developed empirically based methods for modeling the distributions of colluvium and shallow groundwater on landslide-prone hillslopes of Seattle, WA. Tests performed with empirical data not used during model development indicated that the models accurately predicted colluvium and groundwater depths in the region for which they were developed and a second nearby region to which they were applied. The methods we developed should also be applicable in similar regions. For application elsewhere, the individual relations should be modified using empirical data specific to the region of interest.

Our conceptual model of colluvium formation in Seattle is largely based on the idea that hisllslopes that have experienced relatively accelerated slope toe erosion are producing a more mobile layer of colluvium, mainly through landsliding. This increased mobility results in thinner colluvial cover and higher, steeper escarpments at slope crests. Our statistical model accounts for these escarpment characteristics and the gravitational mobility of colluvium as related to slope. Validation of the model indicates that it accurately predicts colluvium thickness, suggesting that our conceptual model is correct. Colluvial groundwater is perched so its depth depends on its saturated thickness, which can be estimated by colluvial basal slope and hydraulic conductivity, and solutions of equations of groundwater flow.

Published in 2007 by John Wiley & Sons, Ltd.

DOI: 10.1002/esp

Perennial groundwater recharge is provided by regional groundwater discharge into colluvium. Significant seasonal recharge is provided by winter precipitation. Historical landslides have been triggered by significant precipitation events and occurred with about equal frequency within and outside of the area affected by of regional groundwater. Regional groundwater conditions appear to have some effect on landslide characteristics; deep landslides are more frequent within the area affected by regional groundwater, while shallow landslides are less frequent within this area.

## Acknowledgements

Kathy Troost (Pacific Northwest Center for Geologic Mapping Studies, PNCGMP) provided geological and geotechnical data and logistical support. Erik Sommargren (formerly of PNCGMP) provided geological and geotechnical data, collaborated with field work and assisted with GIS manipulation. Jeffrey Coe and Dianne Brien (US Geological Survey) and an anonymous reviewer provided constructive reviews of this manuscript.

## References

Baum RL, Chleborad AF, Schuster RL. 1998. *Landslides Triggered by the Winter 1996–97 Storms in the Puget Lowland, Washington*, US Geological Survey Open-File Report 98-239.

Baum RL, Savage WZ, Godt JW. 2002. *TRIGRS – a Fortran Program for Transient Rainfall Infiltration and Grid-Based Regional Slope-Stability Analysis*, US Geological Survey Open-File Report 04-0424.

Booth DB. 1987. Timing and processes of deglaciation along the southern margin of the Cordilleran ice sheet. In *North America and Adjacent Oceans During the Last Deglaciation*, Vol. K-3, Ruddiman WF, Wright HE Jr (eds). Geological Society of America: Boulder, CO; 71–90.

Booth DB, Troost KG, Shimel SA. 2000. *The Quaternary Geologic Framework for the City of Seattle and the Seattle–Tacoma Urban Corridor*, US Geological Survey Final Technical Report.

Booth DB, Troost KG, Shimel SA. 2005. *Geologic Map of Northwestern Seattle (Part of the Seattle North 7.5′× 15′ Quadrangle), King County, Washington*, US Geological Survey Scientific Investigations Map 2903.

Buckler WR, Winters HA. 1983. Lake Michigan bluff recession. *Annals of the Association of American Geographers* **73**(1): 89–110.

Chleborad AF. 2000. *Preliminary Methods for Anticipating the Occurrence of Precipitation-Induced Landslides in Seattle, Washington*, US Geological Survey Open-File Report 00-0469.

Chleborad AF. 2003. *Preliminary Evaluation of a Precipitation Threshold for Anticipating the Occurrence of Landslides in the Seattle, Washington, Area*, US Geological Survey Open-File Report 03-463.

Coe JA, Michael JA, Crovelli RA, Savage WZ, Laprade WT, Nashem WD. 2004. Probabilistic assessment of precipitation-triggered landslides using historical records of landslide occurrence, Seattle, Washington. *Environmental and Engineering Geoscience* **10**(2): 103–122.

Craddock KM. 1999. An evaluation of GIS-based, bedrock topography modeling from water well data, Berks Co., Pennsylvania. *Abstracts with Programs – Geological Society of America* **31**(7): 176.

Cruden DM, Varnes DJ. 1996. Landslide types and processes. In *Landslides, Investigation and Mitigation, Transportation Research Board Special Report 247*, Turner AK, Schuster RL (eds). National Research Council: Washington, DC; 36–75.

Dietrich WE, Reiss R, Hsu M-L, Montgomery DR. 1995. A process-based model for colluvial soil depth and shallow landsliding using digital elevation data. *Hydrological Processes* **9**: 383–400.

Downing J. 1983. *The Coast of Puget Sound*. University of Washington Press: Seattle, WA.

Edil TB, Vallejo LE. 1980. Mechanics of coastal landslides and the influence of slope parameters. *Engineering Geology* **16**: 83–96.

Galster RW, Laprade WT. 1991. Geology of Seattle, Washington, United States of America. *Bulletin of the Association of Engineering Geologists* **28**(3): 235–302.

Gerstel WJ, Brunengo MJ, Lingley WS Jr, Logan RL, Shipman H, Walsh TJ. 1997. Puget Sound bluffs: the where, why, and when of landslides following the holiday 1996/97 storms. *Washington Geology* **25**(1): 17–31.

Godt JW. 2004. *Observed and Modeled Conditions for Shallow Landsliding in the Seattle, Washington, Area*, PhD thesis, University of Colorado, Boulder.

Godt JW, McKenna JP, Lu N. 2003. Unsaturated hydraulic properties of hillslope colluvium derived from glacial sediments in the Seattle, Washington, area determined from open-tube capillary rise tests. *Abstracts with Programs – Geological Society of America* **35**.

Hampton MA, Griggs GB, Edil TB, Guy DE, Kelley JT, Komar PD, Mickelson DM, Shipman H. 2004. Processes that govern the formation and evolution of coastal cliffs. In *Formation, Evolution, and Stability of Coastal Cliffs – Status and Trends*, US Geological Survey Professional Paper 1693, Hampton MA, Griggs GB (eds); 7–38.

Heimsath AM, Dietrich WE, Nishiizumi K, Finkel RC. 1999. Cosmogenic nuclides, topography, and the spatial variation of soil depth. *Geomorphology* **27**: 151–172.

Heimsath AM, Dietrich WE, Nishiizumi K, Finkel RC. 2001. Stochastic processes of soil production and transport: erosion rates, topographic variation and cosmogenic nuclides in the Oregon coast range. *Earth Surface Processes and Landforms* **26**: 531–552.

Hsieh PA, Wingle W, Healy RW. 2000. *VS2DI – a Graphical Software Package for Simulating Fluid Flow and Solute or Energy Transport in Variably Saturated Porous Media*, US Geological Survey Water-Resources Investigations Report 99-4130.

Laprade WT, Kirkland TE, Nashem WD, Robertson CA. 2000. *Seattle Landslide Study*, Internal Report W-7992-01. Shannon and Wilson: Seattle, WA.

Miller DJ. 1991. Damage in King County from the storm of January 9, 1990. *Washington Geology* **19**(1): 28–37.

Miller RD. 1973. *Map Showing Relative Slope Stability in Part of West-Central King County, Washington*, US Geological Survey Miscellaneous-Investigations Report I-0852-A.

Montgomery DR, Dietrich WE. 1994. A physically based model for the topographic control on shallow landsliding. *Water Resources Research* **30**(4): 1153–1171.

Montgomery DR, Greenberg HM, Laprade, WT, Nashem WD. 2001. Sliding in Seattle: test of a model of shallow landsliding potential in an urban environment. In *Land Use and Watersheds, Human Influence on Hydrology and Geomorphology in Urban and Forest Areas*, Wigmosta MS, Burges SJ (eds). American Geophysical Union: Washington, DC; 59–72.

Montgomery DR, Sullivan K, Greenberg HM. 1998. Regional test of a model for shallow landsliding. *Hydrological Processes* **12**: 943–955.

Newcomb RC. 1952. *Ground-Water Resources of Snohomish County, Washington*, US Geological Survey Water-Supply Paper 1135.

Quigley RM, Gelinas PJ, Bou WT, Packer RW. 1977. Cyclic erosion–instability relationships: Lake Erie north shore bluffs. *Canadian Geotechnical Journal* **14**: 310–323.

Roering JJ, Kirchner JW, Dietrich WE. 1999. Evidence for nonlinear, diffusive sediment transport on hillslopes and implications for landscape morphology. *Water Resources Research* **35**(3): 853–870.

Roering JJ, Kirchner JW, Sklar LS, Dietrich, WE. 2001. Hillslope evolution by nonlinear creep and landsliding: an experimental study. *Geology* **29**(2): 143–146.

Savage WZ, Morrissey MM, Baum RL. 2000. *Geotechnical Properties for Landslide-Prone Seattle-Area Glacial Deposits*, US Geological Survey Open-File Report 00-0228.

Schulz WH. 2004. *Landslides Mapped Using LIDAR Imagery, Seattle, Washington*, US Geological Survey Open-File Report 2004-1396.

Schulz WH. 2005. *Landslide Susceptibility Estimated from LIDAR Mapping and Historical Records for Seattle, Washington*, US Geological Survey Open-File Report 2005-1405.

Schulz WH. 2007. Landslide susceptibility revealed by LIDAR imagery and historical records, Seattle, Washington. *Engineering Geology* **89**: 67–87.

Sherrod BL, Bucknam RC, Leopold EB. 2000. Holocene relative sea level changes along the Seattle Fault at Restoration Point, Washington. *Quaternary Research* **54**: 384–393.

Shipman H. 2004. Coastal bluffs and sea cliffs on Puget Sound, Washington. In *Formation, Evolution, and Stability of Coastal Cliffs – Status and Trends*, Hampton MA, Griggs GB (eds), US Geological Survey Professional Paper 1693; 81–94.

Terich TA. 1987. *Living with the Shore of Puget Sound and the Georgia Strait*. Duke University Press: Durham, NC.

Troost KG, Booth DB, Wisher AP, Shimel SA. 2005. *The Geologic Map of Seattle – a Progress Report*, US Geological Survey Open-File Report 2005-1252.

Tubbs DW. 1974. *Landslides in Seattle*, Washington Division of Geology and Earth Resources Information Circular 52: Washington.

Tubbs DW. 1975. *Causes, Mechanisms and Prediction of Landsliding in Seattle*, Ph.D. thesis, University of Washington, Seattle.

Vaccaro JJ, Hansen AJ Jr, Jones MA. 1998. *Hydrogeologic Framework of the Puget Sound Aquifer System, Washington and British Columbia*, US Geological Survey Professional Paper 1424-D.

Vallejo LE, Degroot R. 1988. Bluff response to wave action. *Engineering Geology* **26**: 1–16.

Waldron HH, Leisch BA, Mullineaux DR, Crandell DR. 1962. *Preliminary Geologic Map of Seattle and Vicinity, Washington*, US Geological Survey Miscellaneous Geologic Investigations Map I-354.

Woodward DG, Packard FA, Dion NP, Sumioka SS. 1995. *Occurrence and Quality of Ground Water in Southwestern King County, Washington*, US Geological Survey Water-Resources Investigations Report 92-4098.

Zhou G, Esaki T, Mitani Y, Xie M, Mori J. 2003. Spatial probabilistic modeling of slope failure using an integrated GIS Monte Carlo simulation approach. *Engineering Geology* **62**(3/4): 373–386.